

The effect of altering heat input & torch motion on the grain formation of SS316L material in WAAM

Abdulaziz I. Albannai^{1,2} · Antonio J. Ramirez²

Received: 12 August 2024 / Accepted: 9 December 2024

Published online: 12 December 2024

© The Author(s) 2024 OPEN

Abstract

Wire arc additive manufacturing (WAAM) is an effective technique for producing medium to large-size components, due to its convenience and sustainability in fabricating large-scale parts with high deposition rates, employing low-cost and simple equipment, and attaining high material efficiency. Thus, WAAM attracts different industrial sectors and has experienced great growth, particularly over the last decade to overcome production market's challenges. Consequently, fabricating parts in WAAM, mostly resulted in heterogeneity in microstructure of three different zones towards the buildup direction due to different cooling rates; upper zone (thin surface layer of fine grains), middle zone (undesired large columnar grains covers 90% of the produced part), and lower zone (intermediate columnar grains close to substrate material). Accordingly, producing parts consisting of different zones affect the final component mechanical properties. Therefore, controlling the formation of these zones is a key role in improving WAAM technique. Altering torch motion and cooling rates were found to be effective methods to control the homogeneity of the final component in WAAM.

Keywords GMAW · WAAM · SS316L · Columnar grain formation · Heat input & Torch motion

1 Introduction

A significant branch of additive manufacturing (AM) processes is known as wire-arc directed energy deposition (DED) specifically wire arc additive manufacturing (WAAM) is its simplest subdivision process, which uses wires as the feedstock materials controlled by robots or CNC working system as the main motion mechanism to produce parts layer by layer according to the 3D model design [1–3]. WAAM, established in early 1926, refers to the "Application of electric arc as the heat source to create bulk objects by spraying molten metal onto deposited layers," a concept patented by Baker [4, 5]. The WAAM process has many advantages when compared to other AM processes. High deposition rate, high process flexibility and simplicity, ability to fabricate medium to large complex components, and being economic and environment friendly are the main advantages that make WAAM process a promising manufacturing process in AM [6–8]. Roy et al. highlighted that the key benefits of wire arc additive manufacturing include reduced lead times, minimized material waste, enhanced functionality, tailored tooling for low-volume components, and the capability for multi-material design [9]. Gas metal arc welding (GMAW) is among the most frequently employed welding techniques for WAAM and has been utilized for several decades in applications such as surfacing, cladding, and additive manufacturing [10]. GMAW frequently results in an unstable arc accompanied by spatter, which can negatively impact the WAAM process, leading to welding

✉ Abdulaziz I. Albannai, ai.albannai@paaet.edu.kw | ¹Department of Manufacturing Engineering, College of Technological Studies, Public Authority for Applied Education & Training, Jamal Abdulnasser Street, 70654 Shwuaikh, Kuwait. ²Department of Material Science & Engineering, The Ohio State University, 1248 Arthur E. Adams Drive, Columbus, OH 43221, USA.



defects and diminished product quality. To mitigate this challenge, Cold Metal Transfer (CMT) has been introduced. CMT operates by retracting the welding wire via the reversal of the servo motor, controlled through digital processes. The application of the CMT method in WAAM has demonstrated considerable enhancements in both process and arc stability, a reduction in heat input, the elimination of spatter, and an overall improvement in quality when compared to traditional wire feeding techniques [11, 12]. WAAM process depends on melting and solidifying the material, which fed to the weld pool as a form of wire under an electric arc as a heat source to fabricate a final 3D shape by building up layer above another, in a specific buildup strategy, when melting and solidifying the fed wire [12, 13]. During the deposition process, a moving arc repeatedly acts on the previously placed layer, leading to severe heat accumulation. Thus, producing a high temperature gradient (G) and/or low growth rate (R) after deposition forming a columnar solidified grain microstructure and undesired mechanical properties [14], which are the main drawback of WAAM process and making it conservatively used in different applications [15, 16]. The complex thermal behavior makes the components manufactured by WAAM to have three different zones in the produced part as can be seen in Fig. 1A and each zone has its own grain mode and size Fig. 1B due to different cooling rate [17–19]. The midzone mostly covers more than 90% of the produced area of the final component, and this midzone consists of undesired large and long columnar grains forming toward the heat source buildup direction as Fig. 1C is showing. This issue occurs because of thermal conductivity during the WAAM process transpires predominantly in a single direction, necessitating the dissipation of heat towards

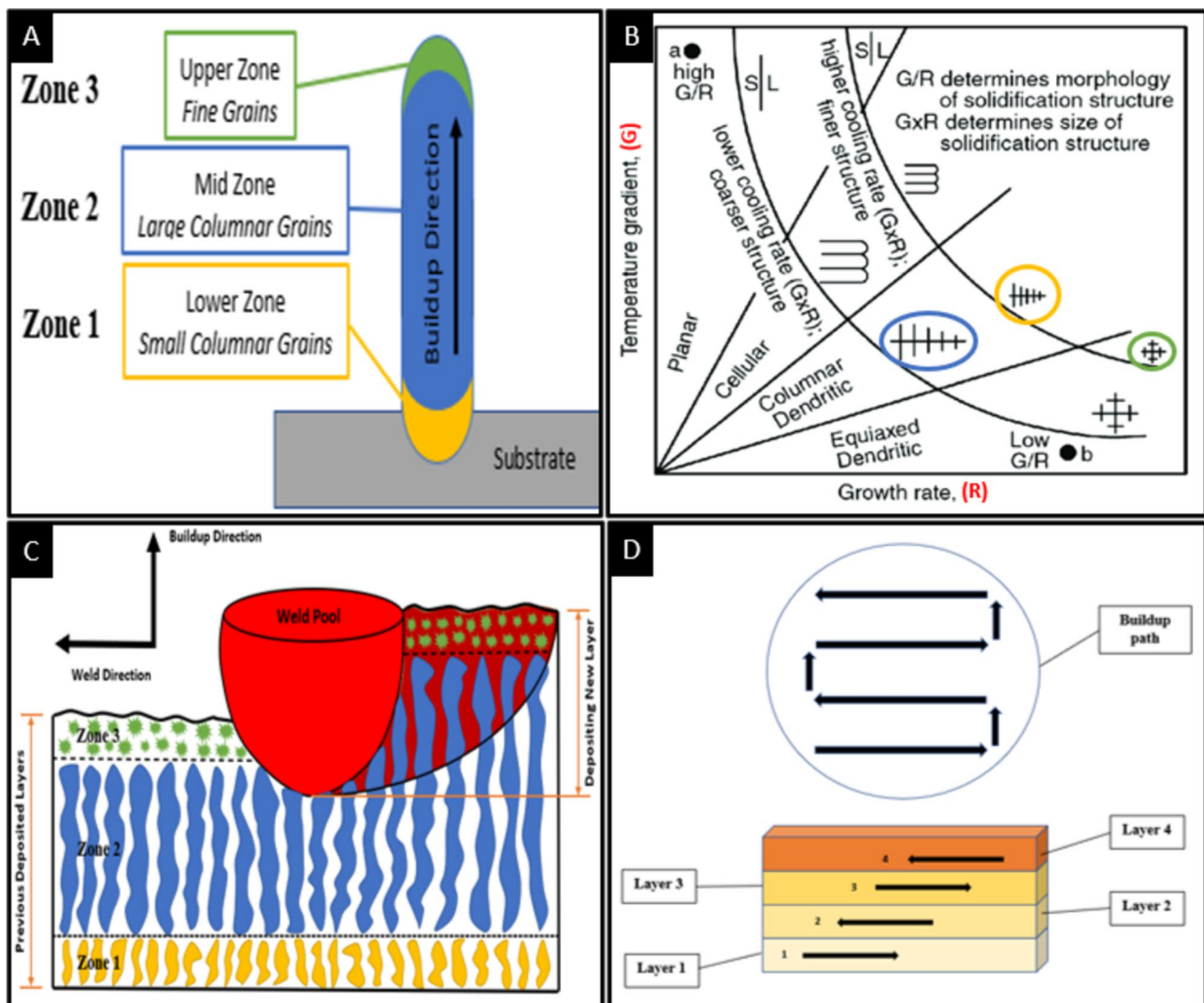


Fig. 1 **A** a schematic of the three different zones forming during WAAM. **B** grain solidification mode related to G and R [19]. The colored circles are the impression of the solidification mode in the three different zones in WAAM. **C** a schematic showing the remelting process during WAAM and the three different zones formation. **D** a schematic of the bidirectional buildup strategy used in this study

Table 1 Composition of the filler metal (ER 316L)

Classification	%C	%Cr	%Cu	%Mn	%Mo	%N	%Nb	%Ni	%P	%S	%Si
Composition	0.15	18.6	0.08	1.7	2.35	0.03	0.01	12	0.02	0.01	0.39

Table 2 The weld parameters used for building different walls

Sample	Travel Speed (mm/min)	Current (A)	Heat Input (J/mm)	Torch Motion-Buildup Strategy
(Base)	1100	110	149	Straight-Bidirectional
1	800	190	205	Straight-Bidirectional
2	400	215	464	Straight-Bidirectional
3	280	240	741	Straight-Bidirectional
4	1100	110	149	Switchback-Bidirectional
5	1100	110	149	Vertical Oscillation-Bidirectional
6	1100	110	149	Spot Like-Bidirectional

the base of the component [10]. Thus, this issue is the critical one found in WAAM process, which forced the industries and researchers around the world to add one or more manufacturing processes to the WAAM in order to improve the final part's microstructure and mechanical properties, which will sacrifice its low-cost advantage and turn the process to be more costly [20]. Some research concluded that the selection of suitable process parameters is essential for attaining a high-quality WAAM structure. Factors such as heat input, cooling rate, and reheating effects significantly influence the morphology, microstructure, and mechanical properties of WAAM components [5, 6, 21]. This study aims to build several walls out of 4 layers above each other using 316L feeding filler wire material with altering heat input and heat source motion in GMAW to improve the process thermal behavior and to form a more homogenous microstructure with smaller grain size rather than heterogenous one with large and longer columnar grains without adding any post or hybrid manufacturing process.

2 Materials & methodology

Build a wall from ER 316L filler wire (which has a chemical composition as received and shown in Table 1 by depositing four layers above each other with best base parameters with bidirectional buildup strategy as can be seen in Fig. 1D using GMAW process (continues arc) to be a (base) sample. Samples (1), (2), and (3) are produced by different heat input and same torch motion as can be seen in Table 2 to be compared with (base) sample and to evaluate the microstructure and the three different zones produced in each wall. On the other hand, samples (4), (5), and (6) are produced by same heat input but applying different torch motion as can be seen in Table 2 to be compared with (base) sample and to investigate the microstructure and the three different zones produced in each wall. All samples were produced using cold metal transfer (CMT) technique for best arc quality, and the metal transfer used in GMAW process was short circuit with tip to work distance of (1.5 mm) and torch angle of (90 degree). The shielding gas used in this study was (98% Argon & 2% Oxygen) with flow rate of (30 l/m). The substrate material used is austenitic stainless steel 316L with dimensions of (200 mm X 100 mm X 12.7 mm). All produced walls have the same unidirectional buildup strategy as can be seen in Fig. 1D and the walls lengths were (90 mm). Sample (4) produced by using switchback torch motion, where the torch was moving forward for (6 mm) and then backward for (3 mm) during the buildup process. Sample (5) produced by using a vertical oscillation torch motion with amplitude of (1 mm), frequency of (4 Hz), and zero dwell time. Sample (6) was produced by a spot-like torch motion, where the torch starts on one location for (0.5 Sec.) then turns off and shifts to the next location (5 mm) linearly away and starts on again so on. Samples (base), (4), (5), and (6) have the same linear speed of (1100 mm/min) and heat input of (149 J/mm). All the produced walls tested on optical microscope after cut, ground, polished, and etched using Beraha's II reagent. The significant results were taken out of an average test of 3 different samples from each wall case from 3 random locations, where the standard deviation has been taken for wall geometry and midzone area percentage, and the possible process improvement will be discussed in this work.

3 Results & discussion

As can be seen in Table 3, the as built (Base) sample of this study showed an average wall size of (4.7 mm) wide and (4 mm) height with (1.7 mm) depth of penetration, which was the smallest wall among of all produced walls, and that is due to lower heat input used. One can clearly see the issue of WAAM process through (Base) sample in both figures Fig. 2-Base and Fig. 3, where long and large columnar grains formed vertically covering the midzone region with almost 95% of total produced wall area. The upper zone of small grains formation has a thin layer almost covering 2% of the total produced wall area due to lower G and faster cooling rate, and the lower zone of small and intermediate columnar grains covering almost 3% only due to faster cooling rate and lower R [22]. The grain solidification mode and size can be understood from both Figs. 1B & 2G, which show the relation among the grain solidification mode formation and the cooling rate with both G & R increasing or decreasing in each zone of the three formed. Comparing (Base) sample with samples (1), (2), and (3) in Fig. 2 showing that increasing the heat input changed the formation of the three zones percentage in each wall. For sample (1) in Fig. 2A showed a reduction in midzone size to cover only 92% of total produced wall area, while the upper and lower zones increased and each covered 4%. Sample (2) in Fig. 2B also showed decreasing in midzone of columnar grains to cover 86% of the total produced wall and the upper and lower zones increased to cover 6% and 8% of total produced area respectively. In sample (3) Fig. 2C the midzone showed the most decreasing percentage among all produced walls samples (Base), (1), (2), and (3) when altering heat input was applied. The midzone of columnar grains covered only 76% in sample (3), while the upper and lower zones covering 11% and 13% respectively. Therefore, increasing the heat input reduced the midzone of large columnar grains, while both the upper zone and lower zones increased. Which proves that changing the heat input manipulates both G and R in each zone and made those zones to form in different amount covering areas and grains mode and size, which agreed with SH Baghjari et al. [19]. Also, there are few important points noticed during increasing the heat input; increasing the heat input led to produce larger grain size in the upper zone proves that G is low as usual but the cooling rate was also lower which means R is reduced too as can be understood from both Figs. 1B & 2G and that is agreed with [15], while in the midzone thinner columnar grains formed as can be seen in sample (3) Fig. 2C in comparison with other samples which shows that both R and G are increased. The change in zones size and the grain size formation related to the change in G and R as can be seen in Figs. 1B & 2G and this finding is in a good agreement with Tiago A. Rodrigues et al. [23] that the thermal cycle acting on lower zone is different from that of the middle or upper zones, because of the heat buildup during production. Moreover, by increasing the heat input a larger wall in size produced in width and height with dipper penetration as can be seen in Fig. 2Base, A, B, & C. For sample (1) the wall width was (6 mm) and the height is (4.7 mm) with a depth of penetration of (2.3 mm). Wall of sample (2) has a width of (9 mm) and a height of (7 mm) with (3 mm) depth of penetration. While sample (3) showed the largest wall produced with a width of (11.4 mm) and a height of (8.6 mm) with (3.5 mm) depth of penetration. Therefore, a good comparison among walls produced by different heat inputs can be seen in Fig. 4A, where one can see the effect of increasing the heat input on the produced wall width to height (W/H) ratio, the midzone percentage, and the depth of penetration. Where (Base) sample showed the best (W/H) ratio of (1.17) since it is the closest to 1 and almost symmetric and it showed the lowest depth of penetration which is desired in WAAM to reduce the remelting process of previous layers, but sample (3) showed the smallest midzone size of large and long columnar grains of only (76%) of total produced area with thinner grains formation. Therefore, heat input found to be main factor for wall geometry in all of width, height, and penetration depth which is agreed with KF Ayarkwa et al. [24].

Table 3 The average wall geometry, midzone covering %, & standard deviation (SD)

Sample	Average Wall Width (SD)	Average Wall Height (SD)	Average Wall W/H Ratio	Average Penetration in (SD)	Average Midzone % (SD)
Base	4.7 mm (0.95)	4 mm (0.13)	1.17	1.7 mm (0.17)	95% (0.22)
1	6 mm (0.88)	4.7 mm (0.25)	1.27	2.3 mm (0.11)	92% (0.1)
2	9 mm (1.2)	7 mm (0.42)	1.29	3 mm (0.31)	86% (0.41)
3	11.4 mm (1.7)	8.6 mm (0.23)	1.32	3.5 mm (0.24)	76% (0.79)
4	7.5 mm (0.54)	6 mm (0.15)	1.25	2.54 mm (0.33)	59% (0.43)
5	5.8 mm (1.66)	6.85 mm (0.71)	0.85	2 mm (1.55)	90% (1.23)
6	8.5 mm (0.78)	8.1 mm (0.25)	1.05	0.35 mm (0.2)	Vanished almost zero% (0.11)

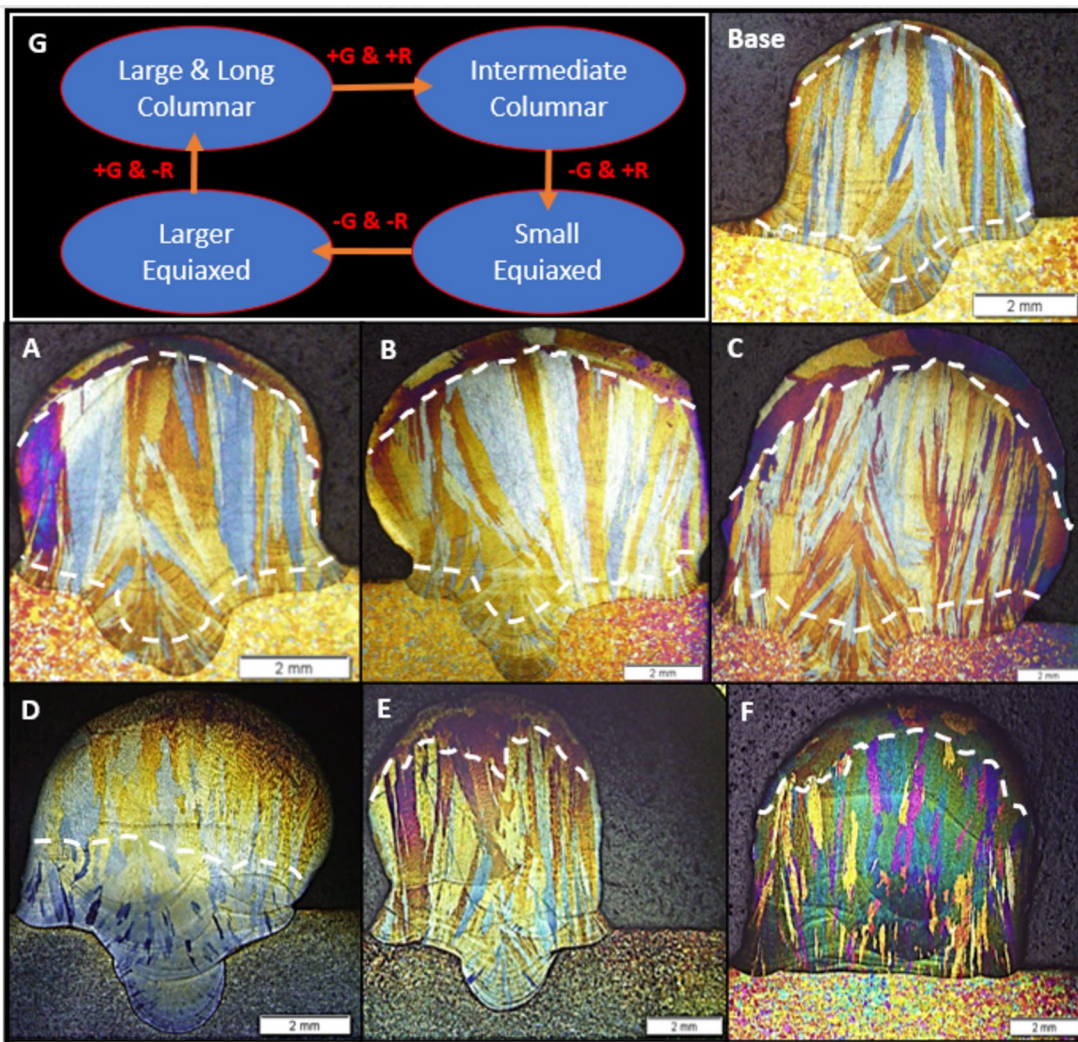


Fig. 2 Showing optical microscope figures for Base) Is the base sample resulted from base weld parameters. **A** Sample (1). **B** Sample (2). **C** Sample (3). **D** Sample (4). **E** Sample (5). **F** Sample (6). While a schematic figure G) showing how the grain mode changes comparing with Fig. 1B

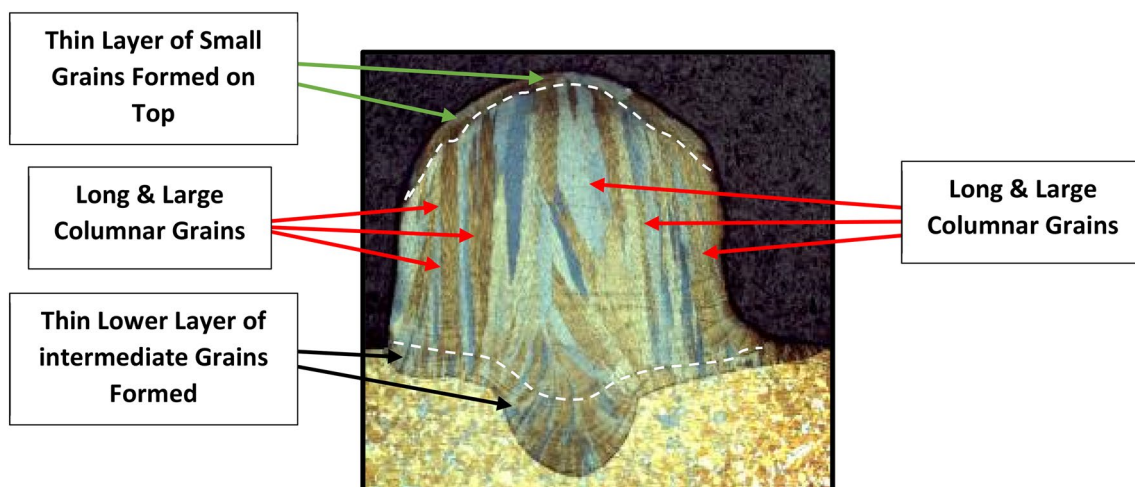


Fig. 3 Showing optical microscope figure for Base sample, where the grains shapes on top differ from the mid-zone and lower zone

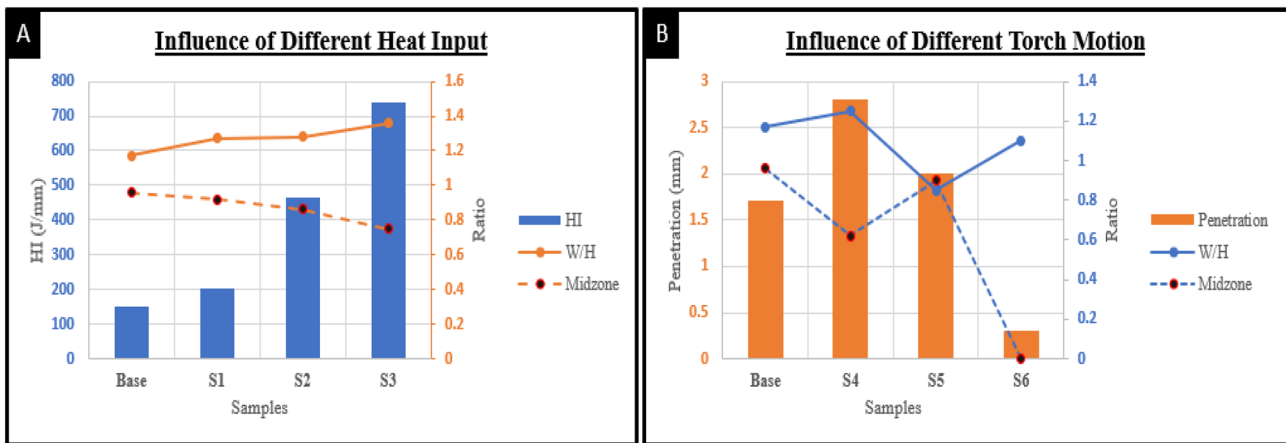


Fig. 4 **A** showing the effect of altering the heat input on both (W/H) ratio and the produced Midzone area percentage. While **B** showing the effect of altering the torch motion on all (W/H) ratio, produced Midzone area percentage, and penetration depth in (mm)

On the other hand, producing walls with variation in torch motion during the buildup strategy showed important results when compared with as built (Base) sample. Using a switchback torch motion produced a wall with only two zones instead of three zones as can be seen in Fig. 2D. The lower zone of small and intermediate columnar grains covering almost 41% of total produced wall area, and the other produced zone with long and large columnar grains covering almost 59%, while no evidence of upper zone been produced in sample (4) and that is resulted from increasing G on surface and decreasing R. Sample (5) in Fig. 2E showed the produced wall of vertical oscillation torch motion in (Z direction), also only two zones formed instead of three zones, but the vanished zone here is the lower zone found in (Base) sample and that proves that the cooling rate was decreased in that region. Thus, the long and large columnar grains zone covered almost 90% of the total produced wall area, and the upper zone of small grains covers only 10%. But the best result found to be in using spot-like torch motion on sample (6) Fig. 2F, and the resulted wall showed almost homogenous microstructure of small and intermediate columnar grains with almost no large or long columnar grains formation compared with all produced walls, and the upper zone covered almost 10%. This achievement showed that rapid cooling, which occurs from switching the arc of at one location and jumping to the next one by a specific overlap distance, affects the microstructure and formed best wall structure. Thus, using spot-like torch motion strategy improves the homogeneity of the produced wall structure, and resisted the growing of the long columnar grains and braked them through the deployed layers vertically. Another fact helped in detached the columnar grains and reduced their length and size, is that using spot-like torch motion has very low penetration and faster cooling rate comparing to all other samples in this study due to shutting off the arc on one location and start on another one with some overlap distance. So, the remelting process in the spot-like torch motion of the previously deployed layer is very low and causes a good barrier for growing the undesired columnar grains toward the buildup direction and shorten them. In general, changing the torch motion can manipulates the three different zones normally found in WAAM process, and the resulted heterogenous microstructure of these three different zones can be improved to produce a wall with almost homogenize microstructure preventing long or large columnar grain formation by applying spot-like torch motion. A clear comparison among all produced walls by different torch motion and by fixing the heat input can be found in Fig. 4B and Table 3, where changing the torch motion influences all (W/H) ratio, the midzone percentage, and depth of penetration. As can be compared to (Base) sample, sample (4) showed a wall width of (7.5 mm) and height of (6 mm) with (W/H) ratio of (1.25), sample (5) showed a wall width of (5.8 mm) and height of (6.85 mm) with (W/H) ratio of (0.85), and sample (6) showed a wall width of (8.5 mm) and height of (8.1 mm) with best (W/H) ratio of (1.05) almost symmetric wall shape. The depth of penetration for samples (4), (5), and (6) were (2.54 mm), (2 mm), and (0.35 mm) respectively.

Also, altering the heat input made significant change in both G and R, which resulted in changing the formation of the three zones percentage and their grain size. Where (G/R) determines the grain solidification mode while (GR) governs the size of the solidification structure [19] and as can be understood from both Figs. 1B & 2G. On the other hand, altering the torch motion produced walls with only two zones instead of three, and by using spot-like torch motion a wall

microstructure without long and large columnar grains was possible to achieve, which found to be agreed with both following equations, Eq. 1. from Moming Ma et al. study [25], and Eq. 2. from Leilei Wang et al. study [26].

$$\lambda = \frac{b}{T} + a, \quad (1)$$

where a & b are alloy's constants, the grain size (λ in μm), and (T in K/s) is the cooling rate [25].

$$\lambda_2 = 50X GR^{(-0.4)} \quad (2)$$

where (λ_2) is the dendritic arms spacing and (GR in K/s) is the cooling rate [26].

4 Conclusions

Producing a wall consisting of four different layers out of austenitic stainless steel material ER 316L filler wire by using a GMAW robotic system as a WAAM process to investigate the effect of different heat input and torch motion during the buildup process on the formation of columnar grains in the produced structure, the following conclusions have been drawn from the current study:

- Applying the WAAM technique to form a wall out of ER 316L filler wire using the GMAW process produced a structure with three different microstructure zones; upper, lower, and middle, which agreed with literature.
- Altering the heat input showed that the formation of these three different zones can be changed in size and grains type due to the change in G and R in each zone.
- Studying different torch motions such as straight, switchback, vertical oscillation, and spot-like proved that forming a wall structure with only 2 different zones is possible.
- With spot like torch motion best wall structure obtained with almost no large or long columnar grains exiting, and the produced grains appear to be smaller and mostly homogenize with almost no penetration.
- The best (W/H) ratio close to (1) which represents the symmetric wall shape, found by applying the spot-like torch motion among all produced walls in this study.
- Future work will be focused on studying the different applications of the spot-like torch motion technique, hopefully forming a full homogenized wall structure in microstructure and mechanical properties.

Acknowledgements The authors thank a Mechanical/Systems Engineer, Mr. Walter Hansen (Department of Center of Design & Manufacturing Excellence (CDME), School of Engineering Science, The Ohio State University) for providing technical support for the robotic system and programing the processes, also for his valuable and helpful technical advice.

Author contributions A.B. wrote the main manuscript text and finalize it and A.R. supervision the research steps and gave the main corrections and guidelines for the paper.

Funding The authors declare that no funds, grants, or other support were received during the preparation of this manuscript.

Data Availability Data sharing is not applicable to this article as no datasets were generated or analyzed during the current study.

Declarations

Competing interests The authors declare no competing interests.

Open Access This article is licensed under a Creative Commons Attribution-NonCommercial-NoDerivatives 4.0 International License, which permits any non-commercial use, sharing, distribution and reproduction in any medium or format, as long as you give appropriate credit to the original author(s) and the source, provide a link to the Creative Commons licence, and indicate if you modified the licensed material. You do not have permission under this licence to share adapted material derived from this article or parts of it. The images or other third party material in this article are included in the article's Creative Commons licence, unless indicated otherwise in a credit line to the material. If material is not included in the article's Creative Commons licence and your intended use is not permitted by statutory regulation or exceeds the permitted use, you will need to obtain permission directly from the copyright holder. To view a copy of this licence, visit <http://creativecommons.org/licenses/by-nc-nd/4.0/>.

References

1. Çam G, Günen A. Challenges and opportunities in the production of magnesium parts by directed energy deposition processes. *J Magnes Alloys*. 2024;12(5):1663–86.
2. Çam G. Prospects of producing aluminum parts by wire arc additive manufacturing (WAAM). *Mater Today*. 2022;62:77–85.
3. Yi H, Wang Q, Cao H. Wire-arc directed energy deposition of magnesium alloys: microstructure, properties and quality optimization strategies. *J Market Res*. 2022;20:627–49.
4. Korzhyk, V., et al. Welding technology in additive manufacturing processes of 3D objects. *Materials Science Forum*. 2017. Trans Tech Publ. 906: 121–130.
5. Jin W, et al. Wire arc additive manufacturing of stainless steels: a review. *Appl Sci*. 2020;10(5):1563.
6. Li Y, Su C, Zhu J. Comprehensive review of wire arc additive manufacturing: Hardware system, physical process, monitoring, property characterization, application and future prospects. *Results Eng*. 2022;13: 100330.
7. Günen A, et al. A new approach to improve some properties of wire arc additively manufactured stainless steel components: simultaneous homogenization and boriding. *Surf Coat Technol*. 2023;460: 129395.
8. Ceritbinmez F, et al. A comparative study on drillability of Inconel 625 alloy fabricated by wire arc additive manufacturing. *J Manuf Process*. 2023;89:150–69.
9. Roy S, et al. Mitigating scatter in mechanical properties in AISI 410 fabricated via arc-based additive manufacturing process. *Materials*. 2020;13(21):4855.
10. Treutler K, Wesling V. The current state of research of wire arc additive manufacturing (WAAM): a review. *Appl Sci*. 2021;11(18):8619.
11. Albannai AI, León-Henao H, Ramirez AJ. Preventing columnar grains growth during hybrid wire arc additive manufacturing of austenitic stainless steel 316L. *Eng Rep*. 2024. <https://doi.org/10.1002/eng2.12914>.
12. Tomar B, Shiva S, Nath T. A review on wire arc additive manufacturing: processing parameters, defects, quality improvement and recent advances. *Mater Today Commun*. 2022;31: 103739.
13. Srivastava M, et al. Wire arc additive manufacturing of metals: a review on processes, materials and their behaviour. *Mater Chem Phys*. 2023;294: 126988.
14. Li S, et al. Controlling the columnar-to-equiaxed transition during Directed Energy Deposition of Inconel 625. *Addit Manuf*. 2022;57: 102958.
15. Arana M, et al. Influence of deposition strategy and heat treatment on mechanical properties and microstructure of 2319 aluminium WAAM components. *Mater Des*. 2022;221: 110974.
16. Kennedy JR, et al. The potential for grain refinement of Wire-Arc Additive Manufactured (WAAM) Ti-6Al-4V by ZrN and TiN inoculation. *Addit Manuf*. 2021;40: 101928.
17. Vora J, et al. Experimental investigations on mechanical properties of multi-layered structure fabricated by GMAW-based WAAM of SS316L. *J Mater Res Technol*. 2022. <https://doi.org/10.1016/j.jmrt.2022.08.074>.
18. Liberini M, et al. Selection of optimal process parameters for wire arc additive manufacturing. *Procedia Cirp*. 2017;62:470–4.
19. Baghjari S, AkbariMousavi S. Experimental investigation on dissimilar pulsed Nd: YAG laser welding of AISI 420 stainless steel to kovar alloy. *Mater Des*. 2014;57:128–34.
20. Rosli NA, et al. Review on effect of heat input for wire arc additive manufacturing process. *J Market Res*. 2021;11:2127–45.
21. Chen X, et al. Microstructure and mechanical properties of the austenitic stainless steel 316L fabricated by gas metal arc additive manufacturing. *Mater Sci Eng, A*. 2017;703:567–77.
22. Xian G, et al. Effect of welding speed on microstructure and anisotropic properties of wire-arc additive-manufactured ti-6al-4v alloy. *Trans Indian Inst Met*. 2023;76(2):483–9.
23. Rodrigues TA, et al. Wire and arc additive manufacturing of HSLA steel: effect of thermal cycles on microstructure and mechanical properties. *Addit Manuf*. 2019;27:440–50.
24. Ayarkwa K, Williams SW, Ding J. Assessing the effect of TIG alternating current time cycle on aluminium wire+ arc additive manufacture. *Addit Manuf*. 2017;18:186–93.
25. Ma M, Wang Z, Zeng X. A comparison on metallurgical behaviors of 316L stainless steel by selective laser melting and laser cladding deposition. *Mater Sci Eng, A*. 2017;685:265–73.
26. Wang L, Xue J, Wang Q. Correlation between arc mode, microstructure, and mechanical properties during wire arc additive manufacturing of 316L stainless steel. *Mater Sci Eng, A*. 2019;751:183–90.

Publisher's Note Springer Nature remains neutral with regard to jurisdictional claims in published maps and institutional affiliations.